Tellus (2004), 56B, 397–403
Printed in UK. All rights reserved

TELLUS

The Arctic: a sink for mercury

By PARISA A. ARIYA[1]*, ASHU P. DASTOOR[2], MARC AMYOT[3], WILLIAM H. SCHROEDER[4], LEONARD BARRIE[5], KURT ANLAUF[4], FARHAD RAOFIE[1], ANDREW RYZHKOV[1], DIDIER DAVIGNON[2], JANICK LALONDE[3] and ALEXANDRA STEFFEN[4],
[1]*Departments of Atmospheric & Oceanic Sciences, and Chemistry McGill University, 801 Sherbrooke Street West, Montreal, PQ, Canada, H3A 2K6;* [2]*Meteorological Service of Canada, Environment Canada, 2121 Route Transcanadienne, Dorval, QC, Canada;* [3]*Département des sciences biologiques, Université de Montréal, 90 Vincent D'Indy, D-223, Montreal, PQ, Canada, H2V 2S9;* [4]*Meteorological Service of Canada, Environment Canada, Toronto, Ontario, Canada, M3H 5T4;* [5]*Environment Division, AREP, World Meteorological Organization, 7 bis, Avenue de la Paix, BP2300, 1211 Geneva 2, Switzerland*

(Manuscript received 30 October 2003; in final form 13 April 2004)

ABSTRACT

Mercury is a persistent, toxic and bio-accumulative pollutant of global interest. Its main mass in the troposphere is in the form of elemental gas-phase mercury. Rapid, near-complete depletion of mercury has been observed during spring in the atmospheric boundary layer of frozen marine areas in Arctic, sub-Arctic and Antarctic locations. It is strongly correlated with ozone depletion. To date, evidence has indicated strongly that chemistry involving halogen gases from surface sea-salt is the mechanism of this destruction. Precisely which halogen gases are the main players has remained unresolved. Our novel kinetic data and multiscale modelling show that Br atoms and BrO radicals are the most effective halogens driving mercury oxidation. The reduction of oxidized mercury deposited in the snow pack back to Hg^0 and subsequent diffusion to the atmosphere is observed. However, it cannot compensate for the total deposition, and a net accumulation occurs. We use a unique global atmospheric mercury model to estimate that halogen-driven mercury depletion events result in a 44% increase in the net deposition of mercury to the Arctic. Over a 1-yr cycle, we estimate an accumulation of 325 tons of mercury in the Arctic.

1. Introduction

It has now been 5 yr since Schroeder et al. (1998) reported surprisingly rapid depletion of mercury vapour from the atmospheric boundary layer during spring ozone depletion events in the high Arctic at Alert (82.5°N, 62.3°W), Canada. Since then, there has been a growing body of observational evidence indicating that $Hg^0_{(g)}$ depletion is widespread in polar regions in the Arctic (Lindberg et al., 2002), Antarctica (Ebinghaus et al., 2002) and the marine sub-Arctic, and is associated with enhanced mercury deposition in surface snow and ice (Lu et al., 2001). Interestingly, nearly complete depletion of ozone in the boundary layer over large areas and evidence of reactive halogens have been observed during most mercury depletion events (MDEs) (Barrie et al., 1988; Barrie and Platt, 1997; Foster et al., 2001; Laurier et al., 2003).

The dominant form of mercury in the atmosphere is elemental mercury ($Hg^0_{(g)}$) which is generally assumed to be long-lived (∼1–2 yr) (Schroeder et al., 1998). Upon reaction with atmospheric oxidants, including halogens, it can be transformed to oxidized compounds (predominantly Hg^{+2} and, in the case of BrO-initiated reactions, Hg^{+2} and Hg^{+1} (Ariya et al., 2002; Raofie and Ariya, 2003). Both Hg^{+2} and Hg^{+1} are more hygroscopic than $Hg^0_{(g)}$, are readily deposited on aerosol or ice and may potentially be assimilated into the food chain upon snowmelt. Indeed, very toxic methyl mercury can be produced from inorganic Hg^{+2} precursors, and can be biomagnified in the human food chain via natural biotic and abiotic processes (AMAP 1998; ATSDR 1999; Takizawa and Osame, 2001). It has become increasingly clear that mere physical processes such as adsorption and condensation of $Hg^0_{(g)}$ on surfaces, including snow and ice-fog crystals, cannot elucidate the magnitude of disappearance of $Hg^0_{(g)}$ in the boundary layer (Lu et al., 2001). Indirect evidence indicates that chemical/photochemical reactions of halogens are involved in mercury destruction and are strongly correlated with ozone depletion chemistry (Lindberg et al., 2002; Laurier et al. 2003; Calvert and Lindberg, 2003). However, until now, the lack of kinetic data has precluded the drawing of any definite conclusions on whether the disappearance of atmospheric mercury

*Corresponding author.
email: parisa.ariya@mcgill.ca

in the Arctic at springtime can cause a net loss of mercury in the troposphere, and whether this may lead to accumulation in terrestrial and aquatic systems. We have now made the kinetic measurements, and we explore their implications in this paper.

2. Methods

2.1. Field measurement of gaseous elemental mercury

Using the automated Tekran Inc. 2537A mercury vapour monitor, operated with 5 or 30 min integrated sampling (preconcentration) time, continuous ground-level measurements of atmospheric gaseous elemental mercury were performed at Alert (Schroeder et al., 1995). Air samples were taken with a heated Teflon line equipped with a 47 mm diameter Teflon filter (0.2 μm pore size) located at the inlet of the sampling line, and a similar filter located at the "sample in" port at the rear of the instrument.

2.2. Snow experiments

We conducted photoinduced Hg(II) reduction experiments by incubating freshly sampled snow in 1 l Teflon bottles under the sun (Lalonde et al., 2002). $Hg^0_{(aq)}$ levels were analysed in snowmelt with a gas-phase atomic fluorescence spectrometer (Tekran 2537). The method uses the 1.5 l min^{-1} flow of the Hg analyser to purge and analyse discrete snowmelt samples, generating near real-time (5 min) data on $Hg^0_{(aq)}$ in samples and blanks. The working detection limit of this method was calculated as $<$0.01 pmol, or three times the standard deviation of 10 system blanks. Volumes of 100 to 350 ml were decanted into a 500 ml glass bubbler and purged for from 10 to 20 min using a zero air generator (Tekran model 1100). Dissolved organic carbon was quantified with a Technicon autoanalyser by persulfate–UV oxidation, followed by conductiometric determination of the CO_2 released.

2.3. Model descriptions

2.3.1. Box model. We used MoccaIce (Model Of Chemistry Considering Aerosols In Cold Environment) to investigate the chemistry of molecular and atomic halogens during the Arctic tropospheric mercury depletion events. Previously used for the marine air at mid-latitudes (Sander et al., 1997), MoccaIce has now been modified to include the chemistry of mercury. MoccaIce contains 157 reactions in the gas phase and 102 in aerosol particles. The number of chemical species is 83 in the gas phase and 68 in the aqueous phase. Since the Arctic air mass is very stagnant during ozone depletion, coinciding mostly with MDEs, the boundary layer can be treated as a "smog chamber" reactor. The reactions of mercury with HO, O_3, Cl_2, Br_2, Cl and Br are parametrized in the model considering the initial attack. The model runs start at Julian day (JD) 90 (JD 1 = 1 January) with initial concentrations set to typical values for the Arctic spring. Emissions of Br_2 and Cl_2 by a marine halogen source were at rates of 17 pmol mol^{-1} day^{-1} and 113 pmol mol^{-1} day^{-1} respectively. Cl and Br radicals were generated upon the photolysis of Cl_2 and Br_2 (Sander et al. 1997). The daytime concentrations of HO, Cl and Br are approximately 10^{-5} cm^{-3}, 10^{-4} cm^{-3} and 10^{-7} cm^{-3} respectively.

2.3.2. Global atmospheric mercury model. At the Meteorological Service of Canada (MSC), we have developed a Global–Regional Atmospheric Heavy Metals Model (GRAHM) which is an Eulerian, multiscale, on-line, high-resolution (horizontally and vertically) general circulation model (Dastoor and Larocque, 2003). The model makes use of uniform global resolution and high-resolution cascading windows to focus on the Arctic region. Dry deposition of elemental, reactive and particulate mercury is treated in the GRAHM model with a detailed dry deposition scheme which is based on multiple resistance theory which is a function of micrometeorological conditions, land-use types, seasons, ground conditions and particle size distribution. The model includes Reactive Gaseous Mercury (RGM) and ice/snow interactions as scavenging of RGM by ice/snow, but heterogeneous chemistry is not treated due to the lack of data. The global domain provides the exchange of large-scale features with the Arctic. Gaseous- and aqueous-phase mercury chemistry, turbulent planetary boundary layer mixing of momentum, heat, moisture and mercury species over land, water and ice/snow, surface-layer processes, gravity wave drag, cloud processes, solar and infrared radiation, deep and shallow convection, dry deposition and revolatilization of mercury species form the set of chemical and physical processes in the model.

3. Results and discussions

Based on the observed high concentration of BrO in the polar troposphere (Richter et al., 1998, 2002; Müller et al., 2002; van Roozendael et al., 2002), particularly during the MDEs, it has been assumed that BrO is a key player in Hg^0 destruction (Lu et al., 2002). We examined the relative importance of BrO, other halogenated species (X/X_2; X = Cl, Br), and non-halogenated Hg^0 oxidants such as HO and O_3, using a detailed chemical box adjusted for the Arctic environment (see Section 2 and Fig. 1a). It incorporated our novel kinetic results of BrO, and other halogens with mercury (Table 1). Similar to the slow reaction of O_3 with Hg^0 (P'yankov, 1949; Schroeder et al., 1995; Hall, 1995; Ariya and Ryzhkov, 2003; Pal and Ariya, 2004), our model simulations indicate that the reactions of Cl_2 and Br_2 with Hg^0 are far too slow to be important atmospheric sinks for mercury (Fig. 1b). Despite the expected decrease in HO production from O_3 photolysis, as a result of the high solar zenith angle and low partial pressure of water vapour in the Arctic atmosphere, model estimates of HO concentration are higher than the values expected from pure gas-phase chemistry (Paterson and Reeh, 2001), hinting at influence of the snow pack (Domine and Shepson, 2002). Hydroxyl

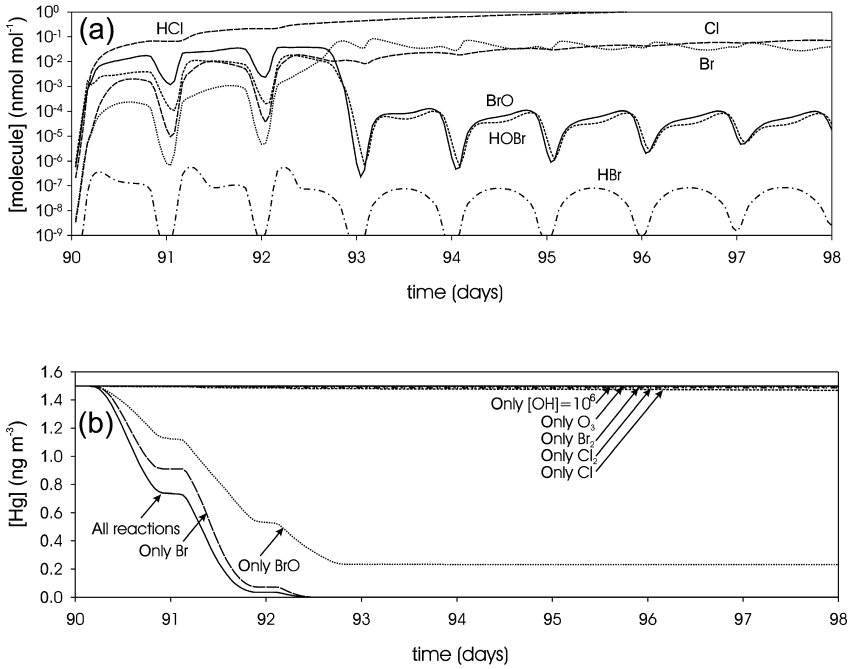

Fig 1. (a) Time-series of selected halogen mixing ratios. (b) Time-series of mercury upon the reactions with HO, O_3, Cl, Br, Cl_2, Br_2, BrO and all reactions.

Table 1. Lifetime of Hg^0 upon reaction with selected atmospheric oxidants at 298 K

Reaction	Rate constant (cm^3 $molecule^{-1}$ s^{-1})	[Oxidant] (cm^{-3})	Lifetime[a] (days)	Reference
$Hg^0 + Cl_2 \rightarrow$ products	$(2.6 \pm 0.2) \times 10^{-18}$	2.5×10^{10}[b]	178	Ariya et al. (2002)
$Hg^0 + Br_2 \rightarrow$ products	$(0.9 \pm 0.2) \times 10^{-16}$	2.5×10^{10}[b]	5	Ariya et al. (2002)
$Hg^0 + Cl \rightarrow$ products	$(1.0 \pm 0.2) \times 10^{-11}$	1×10^4	115	Ariya et al. (2002)
$Hg^0 + Br \rightarrow$ products	$(3.2 \pm 0.4) \times 10^{-12}$	1×10^7	0.40	Ariya et al. (2002)
		1×10^8	0.04	
$Hg^0 + BrO \rightarrow$ products	$10^{-13} < k < 10^{-15}$	7.5×10^{8}[c]	1.03	Raofie and Ariya (2003)
$Hg^0 + O_3 \rightarrow$ products	$(3.0 \pm 2.0) \times 10^{-20}$	7.5×10^{11}	514	Hall (1995)
$Hg^0 + HO \rightarrow$ products	$(8.7 \pm 2.8) \times 10^{-14}$	1×10^5	1330	Sommar et al. (2001)
		1×10^6	133	Sommar et al. (2001)

[a]Lifetime $\tau = (k\ [\text{Oxidant}])^{-1}$, k is a second-order rate constant.
[b]Both Cl_2 and Br_2 are photolysable to atomic Cl and Br at tropospheric solar wavelengths during the polar sunrise and should be considered upper limits.
[c]At 343 K calculated for $k = (1.5 \pm 1.0) \times 10^{-14}$ cm^3 $molecule^{-1}$ s^{-1}.

radical concentrations of 10^5 or 10^6 cm^{-3} could not reproduce mercury depletion events (Fig. 1b). Despite the measured fast rate coefficient of Cl atom-initiated reaction of mercury, the inferred concentration of Cl atoms (Jobson et al., 1994; Ariya et al., 1997) is far too low to play a significant role in the destruction of mercury. The Br atom reaction rate and Br abundance in the atmosphere are sufficient to destroy Hg^0 efficiently within a day. BrO reactions can enhance the impact of Br atoms and shorten the lifetime of mercury, though Br is a more effective oxidant than BrO in Hg^0 destruction (Fig. 1). It is noteworthy that we have carried out sensitivity studies on the values of the rate constants shown in Table 1 to account for the potential uncertainties of the reported values. Modifying the tabulated rate constants by one order of magnitude did not alter the conclusions about the importance of Br and BrO chemistry. Note that the lack of kinetic studies on iodine–mercury reactions precludes evaluation of the impact of iodine compounds at this stage. However, no successful measurement of IO in the Arctic (i.e. the presence of reactive iodine), has been made. There is much evidence indicating that reaction of Hg^0 with halogens and associated ozone depletion occur over seawater, and that mercury-depleted air masses are transported over land afterwards, and hence observed in coastal regions (e.g. Temme et al., 2003). Note that these modelling results do not imply on-site Hg^0 oxidation. Indeed, satellite column

measurements at both poles indicate that BrO concentrations are highest in coastal areas, or over seas, pointing to the required presence of sea ice in BrO formation (Lu et al., 2001; Richter et al., 2002).

Once deposited on snow via Br/BrO oxidation, through photo-oxidation, $Hg^0_{(g)}$ can be produced and recycled back to the atmosphere at the snow/air interface (Lalonde et al., 2002). This phenomenon occurs within hours of deposition and has been observed in suburban and remote temperate locations. We report here that this photoreduction occurs in the high Arctic at Resolute Bay (75°N, 95°W). In low- and high-salinity (20–2000 mg l^{-1}) snow incubated in Teflon bottles under the sun, we observed a rapid photoreduction of about 20 to 21% total Hg within 3 h of exposure, at which time a plateau was reached (Fig. 2). We consider this to be a lower limit, since we only measured Hg^0 in snow not in interstitial air, and some of the newly formed Hg^0 may have migrated from snow to air during incubation. In previous studies in the sub-Arctic, we typically found rapid losses of Hg^0 from the snow pack of the order of 40 to 50% over 48 h (Lalonde et al., 2002, 2003). Since Hg^0 can be oxidized in the snow pack in the presence of sea-salt (Amyot et al., 2003), we anticipate that coastal areas will be more prone to

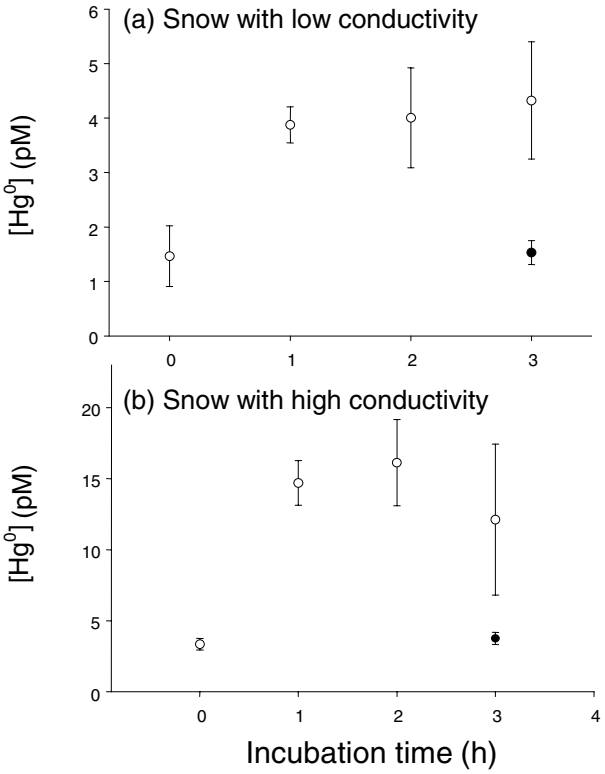

Fig 2. Observed reduction of mercury from the snow pack at (a) low conductivity ($[Cl^-] = 20 \pm 6$ mg l^{-1}) or (b) high conductivity ($[Cl^-] = 1830 \pm 276$ mg l^{-1}), from Resolute Bay. Open circles represent $Hg^0_{(aq)}$ levels in incubation bottles exposed to solar radiation and closed circles represent dark controls.

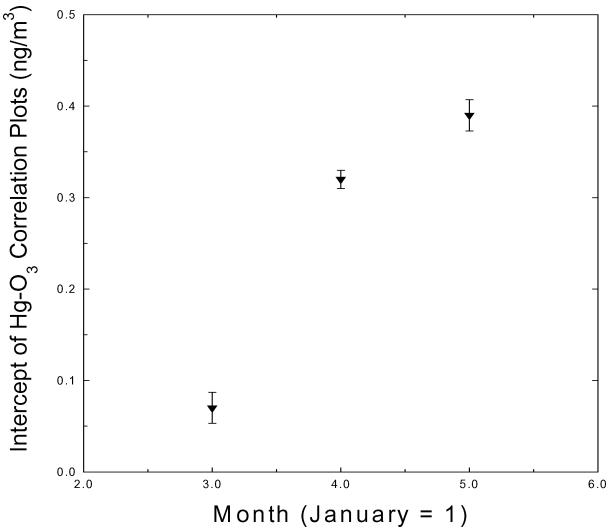

Fig 3. Plots of the intercepts in Hg–O_3 correlation graphs for March, April and May for the period of 1995 to 2001 at Alert based on weekly averaged values from 11 to 216 measurements. The error bars indicate $\pm \sigma/N$.

mercury accumulation than inland regions. Moreover, we analysed 7 yr (1995–2001) of continuous measurement of Hg^0 and ozone at Alert. Correlation plots of ozone and Hg^0 were made with hourly mean data for each month for 7 yr of observations. During March, April and May we observed systematic strong correlations of O_3 and Hg^0($r^2 \geq 0.8$). Our analysis indicates that the revolatilization of deposited mercury is not important in the high Arctic Ocean boundary layer on timescales of several weeks (i.e. the mean time between strong vertical mixing events out on the ice) due to the strong correlation of ozone and mercury depletion at Alert, leading to an intercept close to zero in Hg–O_3 correlation plots (e.g. for the month of April; Fig. 3). However the intercept increases in the late spring (Fig. 3, month of May) where the reduction is enhanced due to an increase in temperature and/or photochemistry.

To investigate the impact of the MDEs on the Arctic environment, we integrated the global atmospheric mercury model GRAHM (see description in Section 2) with and without the presence of MDEs (Figs 4a and b). Space–time distribution and the physical and chemical mechanisms of MDEs in the Arctic boundary layer are introduced into the model based on the observed data, i.e. the lifetime of Hg^0 determined in this study (Table 1), while assuming that these reactions require presence of sea-ice. Without considering the Arctic MDEs, an estimated about 225 tons yr^{-1} total of mercury is deposited in the Arctic (north of 60°N). Inclusion of MDEs in the model increases the total deposition into the MDE region by about 135 tons yr^{-1} (100 tons yr^{-1} inside and 35 tons yr^{-1} outside the Arctic Circle). It thus leads to deposition of 325 tons yr^{-1} in the Arctic. The highest deposition of mercury is observed in the European part of the Arctic, downwind of major anthropogenic source regions,

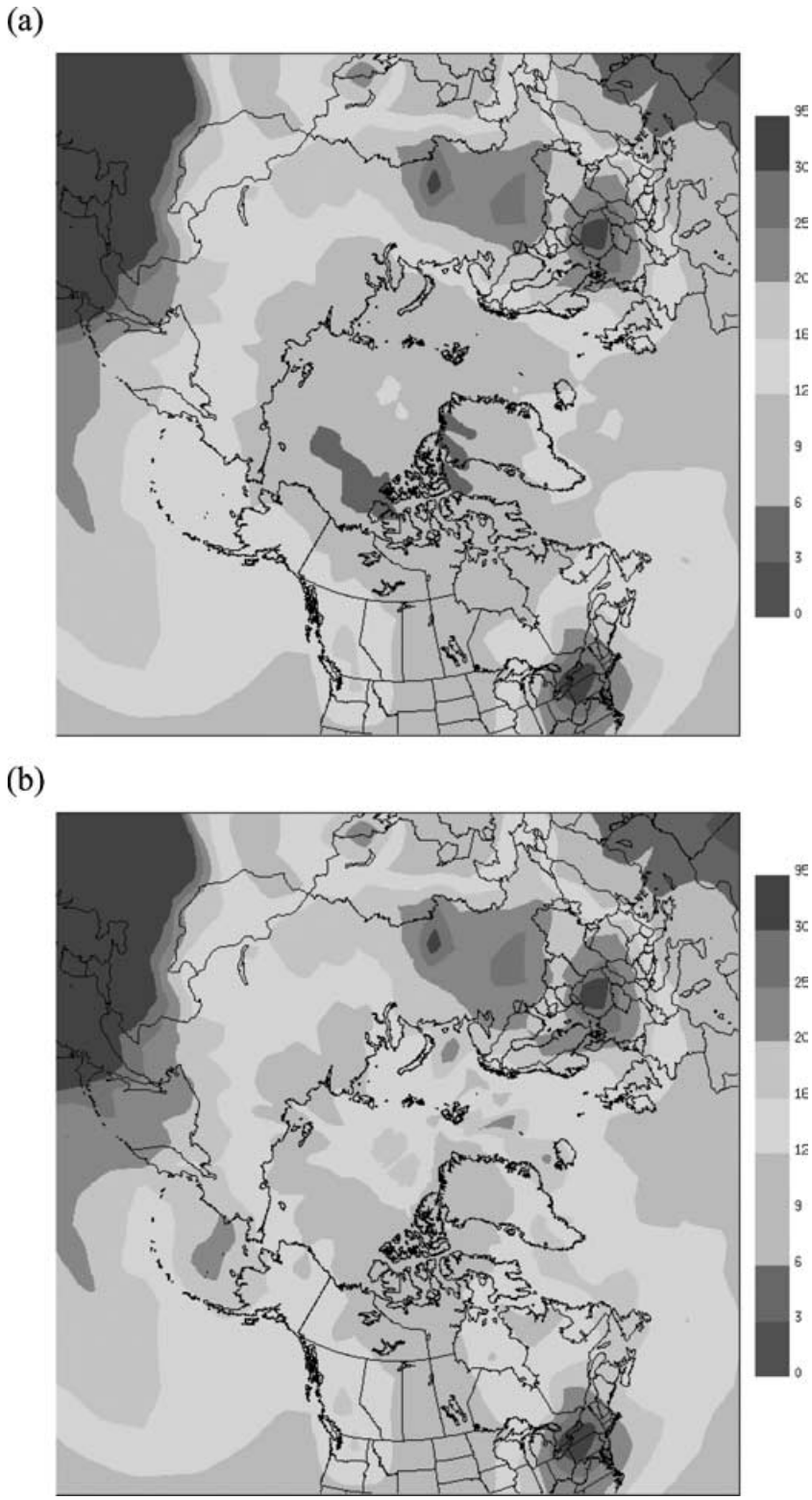

Fig 4. (a) Total annual accumulated mercury deposition (μg m^{-2} yr^{-1}) without the Arctic mercury depletion events (b) Total annual accumulated mercury deposition (μg m^{-2} yr^{-1}) with the Arctic mercury depletion events.

while the lowest depositions are over the Canadian Arctic and Greenland (Fig. 4a). Model results show that the transport of mercury-depleted air masses can contribute to prolonged periods of depletion events in the polar regions, and occasionally they can penetrate over land. The model estimates that almost all of the oxidized mercury during MDEs deposits within the MDE region (+99%). A detailed GCM modelling study including several sensitivity studies will be presented in the near future.

4. Conclusions

We conclude that reactions of Hg^0 with selected halogens, Br and BrO (not Cl, Cl_2 or Br_2), are efficient enough to account for the observed losses of elemental mercury in the Arctic boundary layer. The amount of mercury depletion in the Arctic spring is quite significant and leads to a net loss of gaseous mercury from the atmosphere to the snow surface. Global atmospheric mercury modelling studies show that the Arctic is a sink for mercury, and that MDEs enhance this situation. The mercury products of such a transformation are more hygroscopic, may be readily deposited and could be incorporated in the biota. We acknowledge the complexity of mercury transformation, particularly at the interfaces, and encourage further research into the understanding of mercury chemical speciation and uptake/transformation on snow, ice, interstitial air and interfaces.

5. Acknowledgments

We are very grateful to Jan Bottenheim and Rolf Sander for many helpful suggestions, as well as Caroline Bougie and Clare Salustro for proof reading. We would like to cordially thank NSERC, FCAR, CFI, CFCAS and Environment Canada for financial support.

References

AMAP, 1998. *Arctic Pollution Issues: a State of the Arctic Environment Report*. Arctic Monitoring and Assessment Programme, Oslo.

Amyot, M., Lalonde, J. D., Ariya, P. A. and Dastoor, A. 2003. Behavior of mercury in snow from different latitudes. *J. Phys. IV* **107**, 45–49

Ariya, P. A., Catoire, V., Sander, R., Niki, H. and Harris, G. W. 1997. Trichloroethene and tetrachloroethene: tropospheric probes for Cl- and Br-atom reactions during the polar sunrise. *Tellus* **49B**, 583–591.

Ariya, P. A., Khalizov, A. and Gidas, A. 2002. Reactions of gaseous mercury with atomic and molecular halogens. *J. Phys. Chem. A* **106**, 7310–7320.

Ariya, P. A. and Ryzhkov, A. 2003. Modeling of mercury in the Arctic. *J. Physique IV* **107**, 57–60.

Agency for Toxic Substances and Disease Registry (ATSDR) 1999. *ToxFAQs for Mercury*. Agency for Toxic Substances and Disease Registry, Division of Toxicology, Atlanta, GA. http://www.atsdr.cdc.gov/tfacts46.html

Barrie, L. A., Bottenheim, J. W., Schnell, R. C., Crutzen, P. J. and Rasmussen, R. A. 1988. Ozone destruction and photo-chemical reactions at polar sunrise in the lower Arctic atmosphere. *Nature* **334**, 138–141.

Barrie, L. and Platt, U. 1997. Arctic tropospheric chemistry: an overview. *Tellus* **49B**, 450–454.

Calvert, J. G. and Lindberg, S. E. 2003. A modeling study of the mechanism of the halogen-ozone-mercury homogeneous reactions in the troposphere during the polar spring. *Atmos. Environ.* **37**(32), 4467–4481.

Dastoor, A. P. and Larocque, Y. 2003. Global circulation of atmospheric mercury: a modeling study. *Atmos. Environ.* **38**(1), 147–161.

Domine, F. and Shepson, P. B. 2002. Air–snow interactions and atmospheric chemistry. *Science* **297**, 1506–1510.

Ebinghaus, R., Kock, H. H., Temme, C., Einax, J. W., Löwe, A. G. et al. 2002. Antarctic springtime depletion of atmospheric mercury. *Environ. Sci. Technol.* **36**, 1238–1244.

Foster, K. L., Plastridge, R. A., Bottenheim, J. W., Shepson, P. B., Finlayson-Pitts, B. J. et al. 2001. The role of Br_2 and BrCl surface ozone destruction at polar sunrise. *Science* **291**, 471–474.

Hall, B. 1995. Reactions of ozone with mercury. *Water, Air Soil Pollut.* **80**, 301–315.

Jobson, B. T., Niki, H., Yokouchi, Y., Bottenheim, J., Hopper, F. et al. 1994. Measurements of hydrocarbons during PSE 1992. *Geophys. Res., Atmos.* **99**, 23 355–23 368.

Lalonde, J. D., Amyot, M., Doyon, M. R. and Auclair, J. C. 2003. Photo-induced Hg(II) reduction in snow from the remote and temperate Experimental Lakes area (Ontario, Canada). *J. geophys, Res.* **108**, 4200.

Lalonde, J. D., Poulain, A. J. and Amyot, M. 2002. The role of mercury redox reactions in snow on snow-to-air mercury transfer. *Environ. Sci. Technol.* **36**, 174–178.

Laurier, F. J. G., Mason, R. P., Whalin, L. and Kato, S. 2003. Reactive gaseous mercury formation in the North Pacific Ocean's marine boundary layer: a potential role of halogen chemistry. *J. Geophys. Res.* **108**(D17), 4529, doi:10.1029/2003JD003625.

Lindberg, S. E., Brooks, S., Lin, C.-J., Scott, K. J., Landis, M. S. et al. 2002. Dynamic oxidation of gaseous mercury in the Arctic troposphere at polar sunrise. *Environ. Sci. Technol.* **36**, 1245–1256.

Lindqvist, O., and Rodhe, H. 1985. Atmospheric mercury—a review. *Tellus* **37B**, 136.

Lu, J. Y., Schroeder, W. H., Barrie, L. A., Steffen, A., Welch, H. E. et al. 2001. Magnification of atmospheric mercury deposition to polar regions in springtime: the link to tropospheric ozone depletion chemistry. *Geophys. Res. Lett.* **28**, 3219–3222.

Müller, R. W., Bovensmann, H., Kaiser, J. W., Richter, A., Rozanov, A. et al. 2002. Consistent interpretation of ground based and GOME BrO slant column data. *Adv. Space Res.* **29**, 1655–1660.

Pal, B. and Ariya, P. A. 2004. Kinetics and mechanism of O_3-initiated reaction of Hg^0: atmospheric implication. *J. Phys. Chem. Chem. Phys.* **6**, 572–579.

Paterson, W. S. B. and Reeh, N. 2001. Thinning of the ice sheet in northwest Greenland over the past forty years. *Nature* **414**, 60–62.

P'yankov, V. A. 1949. *Zh. Obsch. Khim.* (Russ. J. Gen. Chem.) **19**, 224–229.

Raofie, F. and Ariya, P. A. 2003. Reactions of BrO with mercury: kinetic studies. *J. Physique IV* **107**, 1119–1121.

Richter, A., Wittrock, F., Eisinger, M. and Burrows, J. P. 1998. GOME observations of tropospheric BrO in Northern Hemispheric spring and summer 1997. *Geophys. Res. Lett.* **25**, 2683–2686.

Richter, A., Wittrock, F., Ladstätter-Weissenmayer, A. and Burrows, J. P. 2002. GOME measurements of stratospheric and tropospheric BrO. *Adv. Space Res.* **29**, 1667–1672.

Sander, R., Vogt, R., Harris, G. W. and Crutzen, P. J. 1997. Modeling the chemistry of ozone, halogen compounds, and hydrocarbons in the arctic troposphere during spring. *Tellus* **49B**, 522–532.

Schroeder, W. H., Keeler, G., Kock, H., Roussel, P., Schneeberger, D. et al. 1995. International field intercomparison of atmospheric mercury measurement methods. *Water, Air Soil Pollut.* **80**, 611–620.

Schroeder, W. H., Anlauf, K. G., Barrie, L. A., Lu, J. Y., Steffen, A. et al. 1998. Arctic springtime depletion of mercury. *Nature* **394**, 331–332.

Sommar, J., Gardfeldt, K., Stromberg, D. and Feng, X. 2001. A kinetic study of the gas-phase reaction between the hydroxyl radical and atomic mercury. *Atmos. Environ.* **35**, 3049–3054.

Takizawa, Y. and Osame, M. (Eds.), 2001. *Understanding of Minamata Disease: Methylmercury poisoning in Minamata and Niigata, Japan*. Japan Public Health Association, Tokyo.

Temme, C., Einax, J. W., Ebinghaus, R. and Schroeder, W. H. 2003. Measurements of atmospheric mercury species at a coastal site in the Antarctic and over the south Atlantic Ocean during polar summer. *Environ. Sci. Technol.* **37**(1), 22–31.

van Roozendael, M., Wagner, T., Richter, A., Pundt, I., Arlander, D. W. et al. 2002. Intercomparison of BrO measurements from ERS-2 GOME, ground-based and balloon platforms. *Adv. Space Res.* **29**, 1661–1666.